



Fast heterogeneous loss of N_2O_5 leads to significant nighttime NO_x removal and nitrate aerosol formation at a coastal background environment of southern China

Chao Yan^{a,b,1}, Yee Jun Tham^{a,b,1}, Qiaozhi Zha^{a,b}, Xinfeng Wang^c, Likun Xue^c, Jianing Dai^a, Zhe Wang^a, Tao Wang^{a,*}

^a Department of Civil and Environmental Engineering, The Hong Kong Polytechnic University, Hong Kong, China

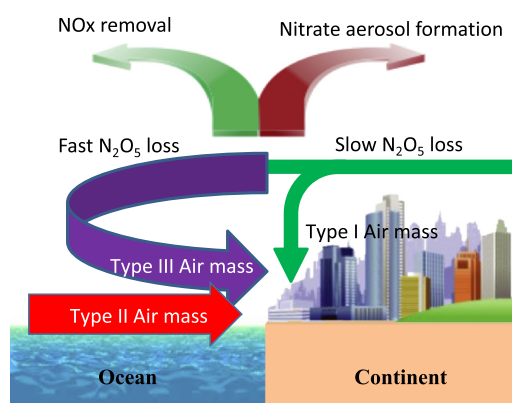
^b Institute for Atmospheric and Earth System Research, Physics, University of Helsinki, 00014, Helsinki, Finland

^c Environment Research Institute, Shandong University, Jinan, Shandong, China

HIGHLIGHTS

- N_2O_5 and NO_3 were observed with distinct features in different airmasses.
- The fast hydrolysis of N_2O_5 dominated the loss of N_2O_5 and NO_3 , particularly when continental air went across the sea.
- The fast loss of N_2O_5 can contribute to a significant fraction of NO_x removal and nitrate aerosol formation.

GRAPHICAL ABSTRACT



ARTICLE INFO

Article history:

Received 10 February 2019

Received in revised form 25 April 2019

Accepted 26 April 2019

Available online 27 April 2019

Editor: Jianmin Chen

Keywords:

Dinitrogen pentoxide

TD-CIMS

N_2O_5 heterogeneous reaction

NO_x removal

Nitrate aerosols

ABSTRACT

Nitrate radical (NO_3) and dinitrogen pentoxide (N_2O_5) play crucial roles in the nocturnal atmosphere. To quantify their impacts, we deployed a thermal-dissociation chemical ionization mass spectrometry (TD-CIMS), to measure their concentration, as well as $ClNO_2$ at a coastal background site in the southern of China during the late autumn of 2012. Moderate levels of NO_3 , N_2O_5 and high concentration of $ClNO_2$ were observed during the study period, indicating active NO_x - O_3 chemistry in the region. Distinct features of NO_3 , N_2O_5 and $ClNO_2$ mixing ratios were observed in different airmasses. Further analysis revealed that the N_2O_5 heterogeneous reaction was the dominant loss of N_2O_5 and NO_3 , which showed higher loss rate compared to that in other coastal sites. Especially, the N_2O_5 loss rates could reach up to 0.0139 s^{-1} when airmasses went across the sea. The fast heterogeneous loss of N_2O_5 led to rapid NO_x loss which could be comparable to the daytime process through NO_2 oxidation by OH, and on the other hand, to rapid nitrate aerosol formation. In summary, our results revealed that the N_2O_5 hydrolysis could play significant roles in regulating the air quality by reducing NO_x but forming nitrate aerosols.

© 2019 Published by Elsevier B.V.

* Corresponding author.

E-mail address: tao.wang@polyu.edu.hk (T. Wang).

¹ These authors have contributed equally to this work.

1. Introduction

Nitrogen oxides ($\text{NO}_x = \text{NO} + \text{NO}_2$), largely emitted by human activities, are key species in a number of atmospheric processes and therefore have crucial impact on climate and human health. In the daytime, NO_x play key roles in regulating ozone formation (Wang et al., 2006; Wang et al., 2010), participating in the formation of highly oxygenated molecules (Yan et al., 2016; Lee et al., 2016) and subsequent formation secondary organic aerosol (Hoyle et al., 2011), as well as leading to direct formation of inorganic nitrate aerosol (NO_3^-) by reacting with hydroxyl radical (OH) to form water soluble nitric acid (HNO_3 , R1), and the R1 has been recognized as the termination of NO_x cycle in the atmosphere (e.g. (Ramanathan et al., 2001))



At night, NO_x can participate in a different set of atmospheric processes. Oxidation of NO_2 by O_3 produces nitrate radical (NO_3 , R2), a major oxidation in the nocturnal boundary layer. It can oxidize various volatile organic compounds (VOC, R3), producing oxygenate products, which can contribute to the formation of organic aerosols (Lucas and Prinn, 2005; Rollins et al., 2009; Ng et al., 2017). Another competing reaction is that NO_3 further reacts with NO_2 to form N_2O_5 , after which NO_3 and N_2O_5 can establish a fast thermal equilibrium (R4, (R4')). N_2O_5 either deposits on aerosol surface through heterogeneous reaction to form inorganic nitrate aerosol (R5) or serves as the reservoir of NO_3 and NO_2 (R4'). If aerosols contain chloride (Cl^-), heterogeneous reaction of N_2O_5 may lead to the formation of ClNO_2 (R6), which can further photolyze to release the chloride radical ($\text{Cl}\cdot$) after sunrise (R7) and affect the atmospheric oxidation capacity (Tham et al., 2014).



These nocturnal processes essentially convert NO_x into nitrate constituents in aerosols, causing a reduction in NO_x and an augment secondary aerosol mass concentration, which however, remain poorly quantified.

A major challenge in estimating the importance of these reactions is the large uncertainty of the N_2O_5 heterogeneous uptake coefficient of N_2O_5 ($\gamma_{\text{N}_2\text{O}_5}$), an important parameter for estimating the N_2O_5 heterogeneous loss rate ($k_{\text{N}_2\text{O}_5}$; see Eq. (1)):

$$k_{\text{N}_2\text{O}_5} = 0.25 \times S_a \times c \times \gamma_{\text{N}_2\text{O}_5} \quad (1)$$

Here, S_a is the surface area of aerosol and c is the molecular velocity of N_2O_5 . Both field and laboratory studies have shown that the $\gamma_{\text{N}_2\text{O}_5}$ values fall between ca. 0.001–0.2. However, the $\gamma_{\text{N}_2\text{O}_5}$ may significantly vary depending on the chemical composition of particles (Brown et al., 2006; Ammann et al., 2013; Brown and Stutz, 2012; Tang et al., 2017). For instance, chloride and water content in the aerosol promote N_2O_5 heterogeneous uptake while, nitrate and organic coating inhibit the heterogeneous uptake of N_2O_5 (Riedel et al., 2012; Tham et al., 2018; Bertram and Thornton, 2009). The mixing status and the diffusive length of the chemical compounds in the aerosol may also play crucial

role in affecting the N_2O_5 heterogeneous uptake (Gaston and Thornton, 2016; Gaston et al., 2014; Ryder et al., 2014). Despite of these new insights, most chemical transfer models derived from the laboratory studies failed to reproduce the field determined $\gamma_{\text{N}_2\text{O}_5}$ (McDuffie et al., 2018), indicating that the complexity of heterogeneous uptake of N_2O_5 remains incompletely understood.

Measurements of N_2O_5 and its loss process either through N_2O_5 heterogeneous reaction or NO_3 loss reactions (term as N_2O_5 reactivity) have been the interest of many field studies in different places around the world over the past decade. For examples, Brown et al. (2003a, 2003b) reported the first simultaneous in situ measurement of a suite of nocturnal nitrogen oxide compounds in Boulder, Colorado, and N_2O_5 reached a peak concentration of nearly 3 ppbv under polluted conditions (Brown et al., 2003a; Brown et al., 2003b). Brown and co-workers then tracked the N_2O_5 reactivity through a flight measurement in New England and found that the N_2O_5 heterogeneous loss dominated the N_2O_5 sink and its lifetime in the polluted airmasses with high sulfate aerosol loading was two orders of magnitude shorter than in relatively cleaner airmasses from eastern Pennsylvania and New Jersey (Brown et al., 2006). A cruise measurement along the United States east coast showed more variation in the N_2O_5 reactivity where N_2O_5 heterogeneous loss dominated the N_2O_5 sink in the outflow airmasses during the night but N_2O_5 loss through the NO_3 sink become more important in airmasses characterized with higher level of terrestrially emitted biogenic VOC (Aldener et al., 2006). Another nighttime aircraft measurement downwind of urban, industrial and rural areas of Texas revealed that the N_2O_5 heterogeneous loss was of less importance (14–28% of the total reactivity) compared to the NO_3 reaction with VOC (Brown et al., 2011). Similar studies were also conducted in Europe, where Crowley et al. (2011) observed at a coastal site in southern Spain that the NO_3 loss reaction was prevailing in the marine airmasses, in contrast to the N_2O_5 -dominated losses in the continental originated airmasses. An airborne N_2O_5 measurement in UK also showed that the N_2O_5 heterogeneous loss was faster than NO_3 loss rate aloft the Southern North Sea, while, the NO_3 loss was dominating in the air above the motorway, Greater London and English Channel (Morgan et al., 2015). As in Asia, Matsumoto et al. (2006) reported that the NO_3 loss accounted for 65–74% of the total loss rate of N_2O_5 in Japan. Recent studies reported intense N_2O_5 heterogeneous uptake and dominating the N_2O_5 loss in the northern polluted regions of China (Tham et al., 2016; Wang et al., 2017a; Wang et al., 2017b; Wang et al., 2017c). These measurements have revealed the spatial variations in the $\text{N}_2\text{O}_5/\text{NO}_3$ reactivity around the world, indicating that the role of N_2O_5 can vary significantly over different environment and airmasses.

Hong Kong, one of the most urbanized coastal cities in Pearl River Delta (PRD), has been suffering from severe photochemical pollutions that are characterized by high mixing ratios of NO_x and O_3 (Wang et al., 2009). Under such circumstances, the importance of N_2O_5 and NO_3 may be amplified in this environment, where pollution is typically distinctive in the airmasses from the inland of China compared to the inflows of marine air (Wang et al., 2003; Wang et al., 2005). Indeed, very high levels of N_2O_5 and ClNO_2 , up to 7.7 and 4.7 ppbv, respectively, were observed at a mountain-top site in Hong Kong (Brown et al., 2016; Wang et al., 2016), and the $\text{NO}_3/\text{N}_2\text{O}_5$ chemistry removed 70% of the NO_x in the nocturnal residual layer and ultimately (Yun et al., 2017), perturbing the NO_x and O_3 level in the next day (Wang et al., 1998). Elevated levels (~2 ppbv) of ClNO_2 were also observed at a coastal and ground-level site (Hok Tsui) in Hong Kong, and the photolysis of ClNO_2 in the early morning led to fast production of Cl atoms, whose oxidative power was several times of that from ozone photolysis (Tham et al., 2014). Continuing that work, this paper analyzes nighttime reactivity N_2O_5 and NO_3 in different airmasses arriving at the coastal site, and discusses the role of N_2O_5 heterogeneous uptake in the NO_x reduction and nitrate aerosol formation.

2. Methods

2.1. Site descriptions

The measurement took place at Hok Tsui atmospheric monitoring station which is located at the southeast tip of Hong Kong Island (22.22° N, 114.25° E). Fig. 1 shows the location of the study site in relation to Hong Kong urban areas and major cities in Pearl River Delta (i.e. Shenzhen, Guangzhou and Macau). The site sits on a 60 m high cliff (above sea level), facing the South China Sea from northeast to the west (~270° view). Hok Tsui is typically in the upwind of the urban cores of Hong Kong and PRD and there are no strong emission sources within the surrounding area (the nearest Hong Kong's urban center is approximately 15 km away), but can be occasionally influenced by urban plumes (e.g. (Wang et al., 1998; Xue et al., 2016)). Therefore, measurements at Hok Tsui station are expected to have a mixture of background characteristics from the ocean and airmasses transported from the urban areas, which is a suitable for investigating the reactivity of NO_3 and N_2O_5 in the different air masses. More detail descriptions of the site can be found elsewhere (Cheng et al., 2000; Wang et al., 2009).

2.2. Measurements

2.2.1. Measurement of $\text{NO}_3 + \text{N}_2\text{O}_5$ and ClNO_2

A thermal dissociation-chemical ionization mass spectrometer (TD-CIMS) was used to measure the $\text{NO}_3 + \text{N}_2\text{O}_5$ and ClNO_2 . A 3 m length of perfluoroalkoxy (PFA) tubing (inner diameter of 9.5 mm; outer diameter of 12.7 mm) was used to draw down the ambient air at a total flow-rate of 6 standard liters per minute (SLPM), leading to a residence time of less than a second. Only 1.55 SLPM out of the total flow was sampled through a 14.8 cm length of heating region (heated at 180 °C) before entering the CIMS while the remaining flow was dumped. The N_2O_5 was thermal-dissociated into NO_3 by the high inlet temperature, while the ClNO_2 would be able to pass through the heating region (Thaler et al., 2011), and subsequently ionized by the reagent ions (iodide, I^-) to produce NO_3^- ions (detected at 62 m/z), and $\text{I}(\text{ClNO}_2)^-$ ions, detected at 208 m/z (Kercher et al., 2009; Slusher et al., 2004). During the campaign, the instrument background was determined hourly by adding a small flow of high concentration of NO (~1000 ppm) into the top of the sampling inlet, in order to 'titrate' the NO_3 and N_2O_5 , ultimately. The TD-CIMS

was calibrated weekly and the average sensitivity during the campaign was determined to be 1.9 ± 0.1 Hz/pptv 0.44 ± 0.05 Hz/ppt (mean \pm standard deviation) for $\text{NO}_3 + \text{N}_2\text{O}_5$ and ClNO_2 , respectively. The detection limit (1 min average, 3σ) was estimated to be 10 pptv and 2 pptv for $\text{NO}_3 + \text{N}_2\text{O}_5$ and ClNO_2 , respectively. The detail sampling, detection, calibration procedures can be found in elsewhere (Wang et al., 2014; Tham et al., 2014).

It has been found that the co-existence of peroxy acetyl nitrate (PAN) and NO_x caused an overestimation of $\text{NO}_3 + \text{N}_2\text{O}_5$ signals (62 m/z) in the daytime (Wang et al., 2014), but such interference was insignificant during the nighttime at Hok Tsui due to relatively low level of PAN and NO_x . Therefore, only nighttime data (19:00–06:00, local time) were extracted for the analysis and the correction of such interference at the nighttime 62 m/z data was estimated to be smaller than 15%. Another uncertainty of this measurement is that the potential loss of N_2O_5 on the inlet surface (i.e., conversion to ClNO_2) might be enhanced when particles deposited on the wall of inlet tube over time. To avoid the large uncertainty from inlet chemistry, only the data from 23 August to 19 September 2012 were used in this study. Upon checking on the ambient data during the instrument background measurements (flooding the inlet with high NO concentration), there is no significant reduction in the ClNO_2 signal, whereas the $\text{NO}_3 + \text{N}_2\text{O}_5$ signal immediately dropped to zero level. This observation suggests that the inlet chemistry (conversion of N_2O_5 to ClNO_2 on inlet surface) was insignificant, at least in this selected study period.

2.2.2. Auxiliary measurements

In addition to TD-CIMS, other ancillary measurement included the routine gases and meteorological parameters. O_3 was measured with a commercial UV photometric analyzer (Model 49i, Thermo Environmental Instruments TEI, USA). NO_x (NO and NO_2) was measured with a chemiluminescence instrument (Model 42i, TEI) equipped with a photolytic NO_2 -converter (Air Quality Design, USA), which is more suitable for measurement in rural site (Xu et al., 2013). The ambient temperature and relative humidity (RH) were monitored with a temperature/RH probe (Model 41382VC/VF, M.R. YOUNG, USA). Wind speed and direction were monitored using a wind monitor (Gill, UK). Photolysis rate of NO_2 was obtained using a filter radiometer (Meteorologie consult gmbh). All of the inlets and meteorological probes/sensors were installed close to each other to reduce inhomogeneity of the sample air.

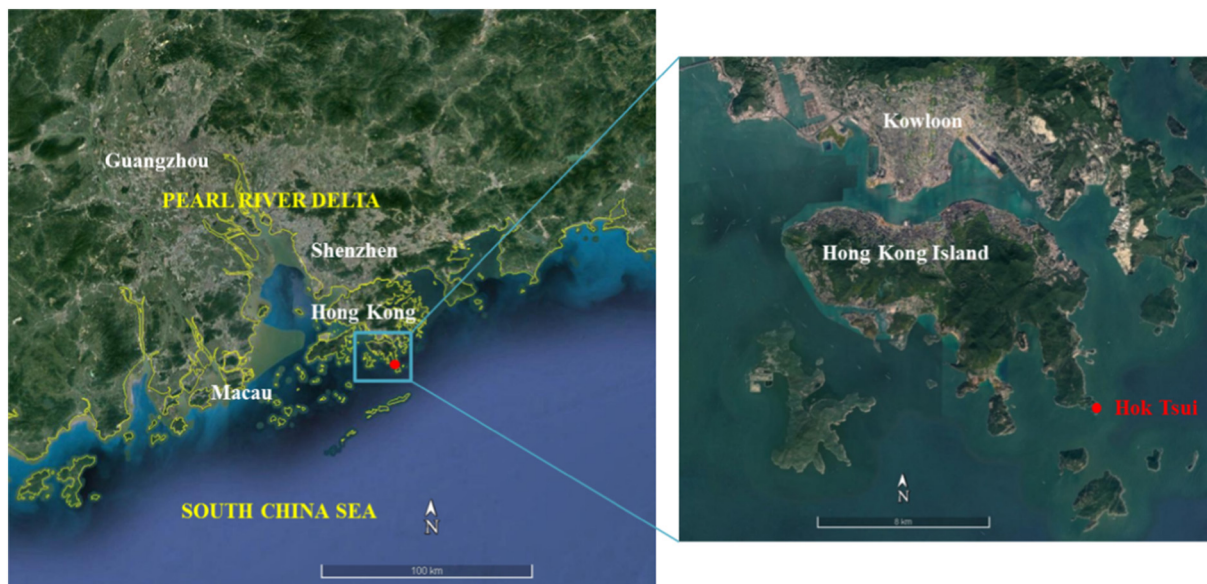


Fig. 1. The location of Hok Tsui site in relative to the urbanization areas in Pearl River Delta, China.

2.3. Estimating the steady-state NO_3 and N_2O_5 loss rates

N_2O_5 can achieve fast thermal equilibrium with NO_3 and NO_2 in ambient condition and can be described by using Eqs. (2) and (3).

$$[\text{N}_2\text{O}_5] = K_{\text{eq}}[\text{NO}_2][\text{NO}_3] \quad (2)$$

$$K_{\text{eq}} = k_4/k_4' \quad (3)$$

Here, K_{eq} is the thermal equilibrium, k_4 and k_4' are the rate constant from R_4 and R_4' , respectively; $k_4 = 1.9 \times 10^{-12} (\text{T}/300)^{0.2} \text{ cm}^3 \text{ molecule}^{-1} \text{ s}^{-1}$ (Viggiano et al., 1981) and $k_4' = 9.7 \times 10^{14} (\text{T}/300)^{0.1} \exp^{-11,080/\text{T}} \text{ s}^{-1}$ (Hahn et al., 2000). With the known $K_{\text{eq}}[\text{NO}_2]$, we can then calculate the N_2O_5 to NO_3 ratio and separate the measured total $\text{NO}_3 + \text{N}_2\text{O}_5$ into individual concentrations of NO_3 and N_2O_5 for further analysis.

Brown et al. (2003a, 2003b) proposed a statistical method to derive the steady-state loss rates of NO_3 and N_2O_5 , based on the field measured NO_2 , O_3 , NO_3 and N_2O_5 . Briefly, the production starts in R_1 , production of $\text{NO}_3 = k_1[\text{NO}_2][\text{O}_3]$. If the NO_3 and N_2O_5 are both in steady-state condition, where their total formation rate and total loss rate are in equivalent, the equation can be shown as in Eq. (4).

$$k_1[\text{NO}_2][\text{O}_3] = k_{\text{NO}_3}[\text{NO}_3] + k_{\text{N}_2\text{O}_5}[\text{N}_2\text{O}_5] \quad (4)$$

where, the k_{NO_3} and $k_{\text{N}_2\text{O}_5}$ denote the first-order loss rates for NO_3 and N_2O_5 , respectively. It should be note that Eq. (4) only holds when NO_3 and N_2O_5 are pseudo steady state, i.e., the production and loss of NO_3 and N_2O_5 are much faster than their net changes.

The steady-state lifetime of NO_3 , $\tau(\text{NO}_3)$, can be calculated from Eq. (5), and the inverse lifetime of NO_3 ($\tau(\text{NO}_3)^{-1}$), also known as the total loss rate, can be redefined as in Eq. (6).

$$\tau(\text{NO}_3) = \frac{[\text{NO}_3]}{k_1[\text{NO}_2][\text{O}_3]} = \frac{[\text{NO}_3]}{k_{\text{NO}_3}[\text{NO}_3] + k_{\text{N}_2\text{O}_5}[\text{N}_2\text{O}_5]} \quad (5)$$

$$\tau(\text{NO}_3)^{-1} = k_{\text{NO}_3} + K_{\text{eq}}[\text{NO}_2] k_{\text{N}_2\text{O}_5} \quad (6)$$

From Eq. (6), the inverse of NO_3 lifetime can be described as a linear function of $K_{\text{eq}}[\text{NO}_2]$. The $\tau(\text{NO}_3)^{-1}$ and $K_{\text{eq}}[\text{NO}_2]$ were obtained from the measurement and the k_{NO_3} and $k_{\text{N}_2\text{O}_5}$ were determined by fitting the slope and intercept of the function.

As has been mentioned, this analysis assumes the steady-state of NO_3 and N_2O_5 , which however, may not hold under some circumstances. For example, if the measurement location is too close to the emission source, the equilibrium may not be established and/or there is insufficient time to achieve steady-state. Here, we used a simple box model to test the validity of steady-state assumption for our measurement. In this model, R_2 , R_4 , and (R_4') were used as the production of NO_3 and N_2O_5 , whereas k_{NO_3} and $k_{\text{N}_2\text{O}_5}$ determined from the field measurement were used to describe the total first-order loss rates of NO_3 and N_2O_5 , respectively, regardless of detailed loss pathways. According to the selected case studies in Section 3.2 below, four sets of initial input parameters were tested. The initial concentrations of NO_3 and N_2O_5 were set to zero, and a nighttime mean temperature of 300 K was used in these runs. The model results of these four cases are presented in Fig. 2. In all of the four cases, after fast accumulations at the beginning, the NO_3 and N_2O_5 slowly decrease, indicating a relatively small net changing rate. Also showed in the bottom two panels of the sub-figures that the net variations of NO_3 and N_2O_5 become much smaller than their production and loss rates after a short period (c.a. 15 min), suggesting that both of them are in pseudo steady-state. As the distance from the nearest major NO_x emission source was approximately 15 km away and with a maximum wind speed of 5 m s^{-1} , a minimum of 50 min was required for the air plume to reach the measurement site,

which is probably enough for NO_3 and N_2O_5 to achieve steady-state for all of our selected cases.

2.4. Calculation of OH concentration

The OH concentration was calculated according to the Ehhalt and Rohrer (2000) parameterization, which based on the function of NO_2 mixing ratio, and the photolysis rates of O_3 and NO_2 .

$$[\text{OH}] = 4.1 \times 10^9 \times (J_{\text{O}_3})^{0.83} (J_{\text{NO}_2})^{0.19} \frac{140[\text{NO}_2] + 1}{0.41[\text{NO}_2]^2 + 1.7[\text{NO}_2] + 1} \quad (7)$$

The J_{NO_2} is the photolysis rate of NO_2 (from filter radiometer measurement), while J_{O_3} , photolysis rate of O_3 , was estimated from the Tropospheric Ultraviolet and Visible (TUV) Radiation Model and then scaled by the measured J_{NO_2} . This parameterization was developed for the summertime conditions (in Germany) with high solar intensity, relative humidity, and biogenic VOC emissions, which are quite similar to the conditions in Hong Kong, but, uncertainty may arise if photolysis of nitrous acid (HONO) is the predominant OH source. The calculated values were consistent with those measured in PRD region and modeled OH concentrations at this site (Li et al., 2018; Hofzumahaus et al., 2009), therefore, may serve as the simplified reference of OH levels in this study.

3. Results & discussion

3.1. Observation of NO_3 , N_2O_5 and ClNO_2

Fig. 3 shows the time-series of NO_3 , N_2O_5 , and ClNO_2 together with related trace gases and meteorological parameters for period between 23 August and 19 September 2012. Similar to the previous observations at this location (e.g. Wang et al., 2003; Wang et al., 1998), abundant of NO_x (up to 51 ppbv) and O_3 (up to 152 ppbv) were observed during the measurement period. These high levels of NO_x and O_3 lead to the active NO_x - O_3 oxidation, thus, significant of NO_3 was observed starting from sunset and decrease at sunrise, with an average nighttime concentration of $7 \pm 12 \text{ pptv}$ (mean \pm standard deviation). Concurrently, N_2O_5 was observed to have a mean nighttime concentration of $17 \pm 33 \text{ pptv}$, with a maximum of 336 pptv observed on the night of 23–24 August 2012. ClNO_2 , a product from the N_2O_5 heterogeneous reaction, was observed with an average night-time concentration of $112 \pm 218 \text{ pptv}$ and can reach up to 2000 pptv during the measurement period, suggesting that there are active N_2O_5 heterogeneous processes in the region. The detail observations of ClNO_2 at this site have been reported in our previous study (Tham et al., 2014).

The higher mixing ratios of NO_3 , N_2O_5 and ClNO_2 observed at the site are typically corresponding to the northerly wind (see wind direction in Fig. 3), which suggest that the polluted airmasses are coming from the urban-cores of Hong Kong and PRD regions. Detailed analysis of 24-h back trajectories calculated by Hybrid Single-Particle Lagrangian Integrated Trajectory (HYSPPLIT) model (Draxler and Hess, 1998) for the measurement period reveal that the airmasses arriving at the measurement site alternately originated from the continent regions (urban areas of Hong Kong and PRD) and the sea (South China Sea). For instance, airmasses were originated from the continent regions in between 23 and 26 Aug 2012 (refer as Type Ia), and then shifted to marine origins from 29 August to 14 September 2012 (Type II) before turning into the continent origins from 15 to 20 September 2012 (Type Ib). There are specific days on 27–28 August 2012 and 18–19 September 2012 that have a mixture of continent and marine airmass, where the continental air moved onto the sea (staying on the sea for $>12 \text{ h}$) before arriving at our measurement site (Type III).

Table 1 summarizes the mean concentration for N_2O_5 , NO_3 , ClNO_2 , O_3 and NO_2 and the lifetime of NO_3 and N_2O_5 in different type of

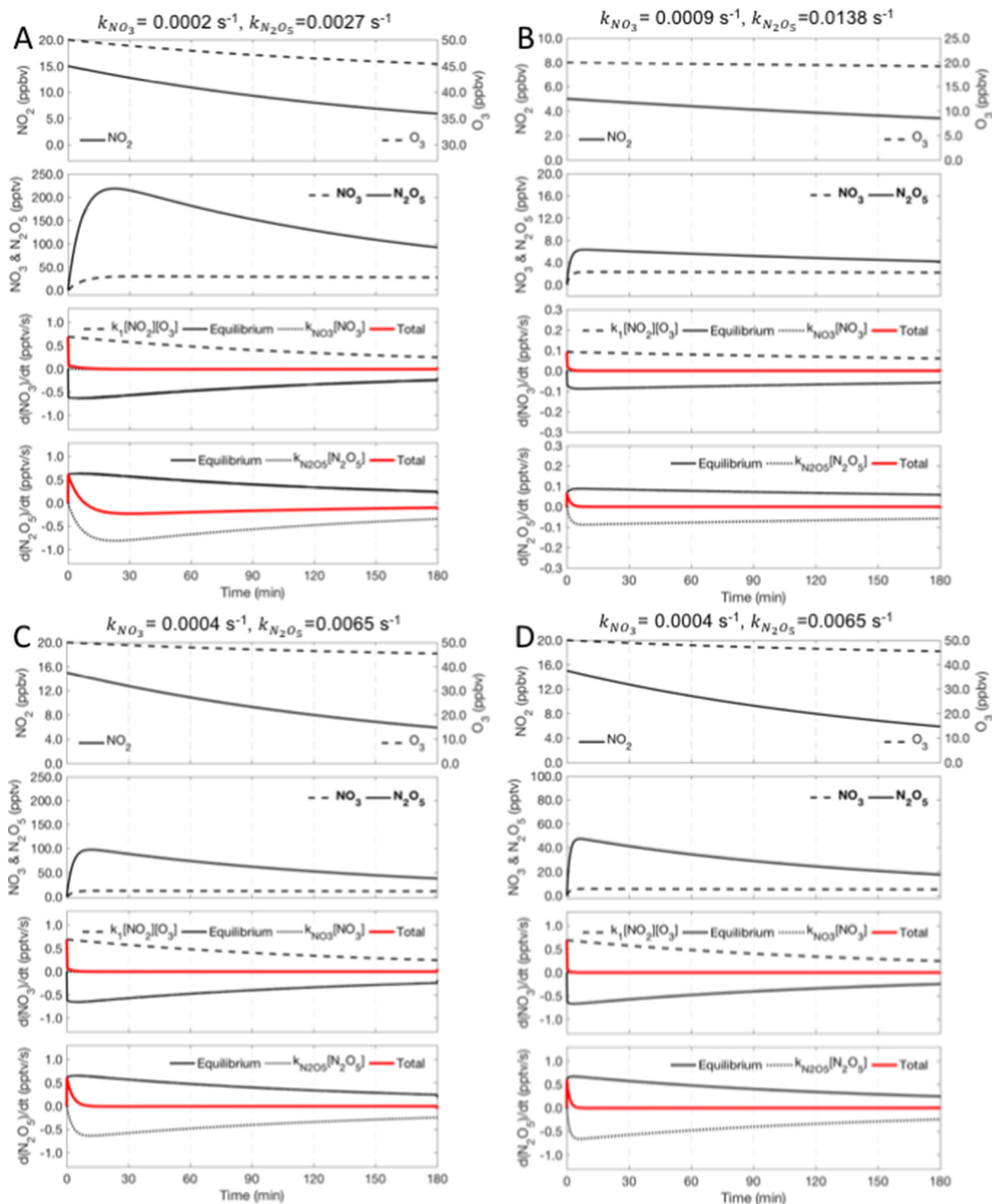


Fig. 2. Verifying the steady-state of NO_3 and N_2O_5 . Model input parameters in A–D are obtained from the four cases shown in Section 3.2.

airmasses. Owing to the high concentrations of precursors (i.e. NO_2 and O_3), highest mixing ratios of NO_3 , N_2O_5 and ClNO_2 were measured in the continental airmasses, in contrast to their lowest concentrations observed in the pristine marine airmasses (typically close to detection limits). The mixture of continent and marine airmass, on the other hand, has moderate concentrations of NO_3 , N_2O_5 and ClNO_2 , although NO_2 and O_3 were similar to the continental airmasses. The lifetime of N_2O_5 (and NO_3 due to their internal equilibrium) in all types of masses were notably shorter than those in the earlier studies in US and Europe (e.g. Brown et al., 2006; Crowley et al., 2011; Morgan et al., 2015; Brown

et al., 2009), especially in Type III airmasses, which suggested fast losses of N_2O_5 and NO_3 at this location. In addition, higher ratios between ClNO_2 and N_2O_5 were found in marine-involved airmasses, indicating more active N_2O_5 heterogeneous chemical processes, probably on the chloride-rich marine aerosols.

3.2. N_2O_5 and NO_3 reactivity

With the observations of short N_2O_5 lifetimes, it is crucial to assess the dominant loss pathway of N_2O_5 , either through NO_3 loss reactions

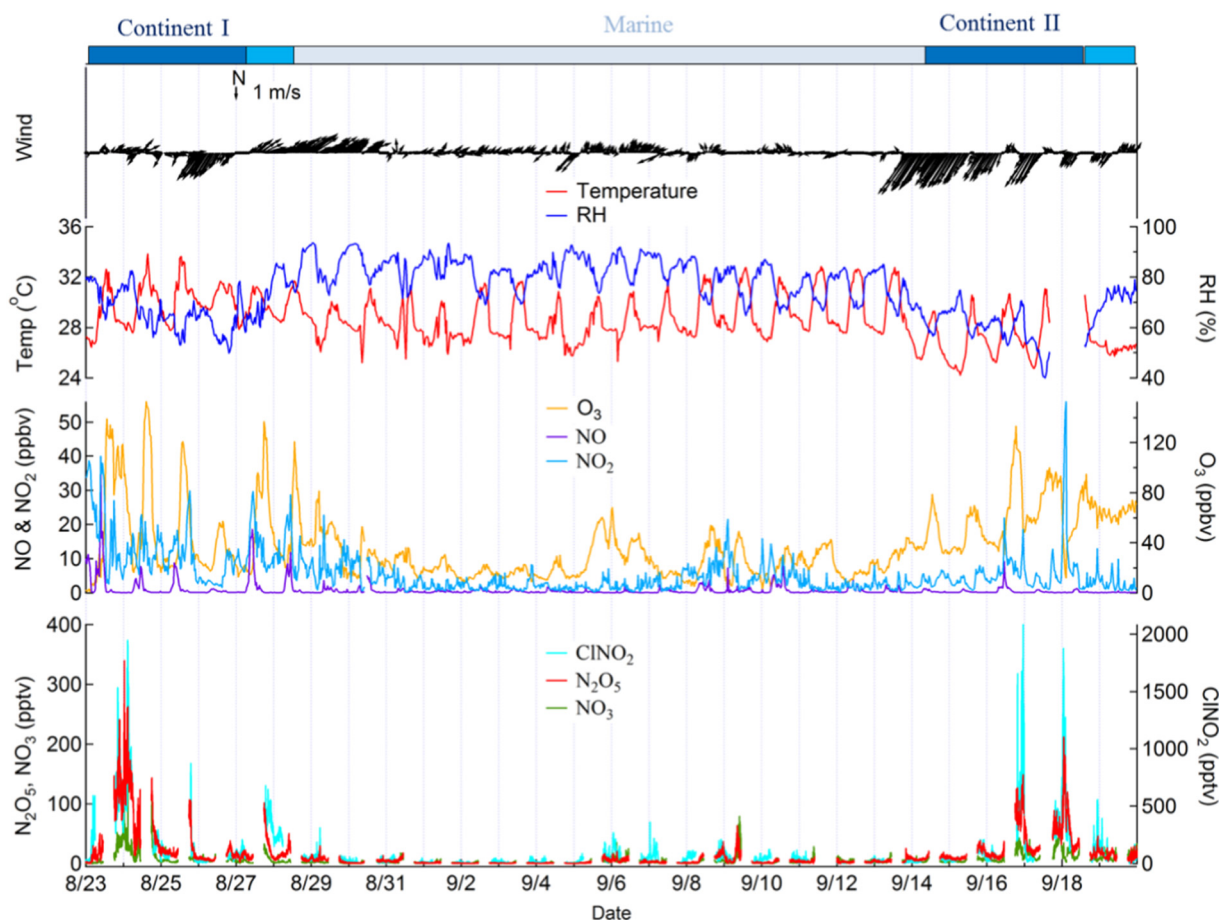


Fig. 3. Temporal variations of meteorological parameters (wind, temperature, and RH), trace gases (CO , O_3 , NO , and NO_2), as well as the sum of NO_3 and N_2O_5 and ClNO_2 . Since this technique detects the sum of $\text{NO}_3 + \text{N}_2\text{O}_5$, the air masses origins were determined from the 48 h back trajectories derived from HYSPLIT.

or N_2O_5 heterogeneous uptake, in order to further determine its importance in the atmospheric processes. We distinguished the N_2O_5 reactivity by evaluating the loss rate of NO_3 and N_2O_5 predicted by the steady-state method described in Section 2.3. As aforementioned, this method may not be valid if the N_2O_5 is not in steady-state or the plume changes throughout the night, which may result in a negative intercept value. Therefore, we carefully selected the valid time period of N_2O_5 data for four different nights to represent the determined types of air masses, namely on 24 August, representing continent air mass (Type Ia); on 9 September, representing air mass origin from marine (Type II); 16 September, representing another continent air mass (Type Ib); and the

night of 18 September represents the mixture of continent and marine air mass (Type III).

Fig. 4 depicts the 24-h air mass back trajectories for the selected four cases, and the loss rates of NO_3 and N_2O_5 in these air masses. The results revealed that the N_2O_5 heterogeneous loss was overwhelming the loss through the NO_3 reactions. The $k_{\text{N}_2\text{O}_5}$ were determined to be 0.0027 s^{-1} , 0.0138 s^{-1} , 0.0065 s^{-1} , and 0.0139 s^{-1} in the Type Ia, Type II, Type Ib and Type III air masses, respectively. The determined k_{NO_3} were more than one order of magnitude smaller, derived to be 0.0002 s^{-1} for Type Ia, 0.0009 s^{-1} for Type II, and 0.0004 s^{-1} for both Type Ib and Type III. The predominant loss pathway for N_2O_5

Table 1
Mean nighttime values (\pm standard deviation, 1σ) for the concentration of N_2O_5 , NO_3 , ClNO_2 , O_3 , and NO_2 , together with N_2O_5 steady-state lifetime and ClNO_2 to N_2O_5 ratio in different type of air masses.

Air mass	Period	N_2O_5 (pptv)	NO_3 (pptv)	ClNO_2 (pptv)	NO_2 (ppbv)	O_3 (ppbv)	$\tau(\text{N}_2\text{O}_5)^a$ (s)	$\text{ClNO}_2/\text{N}_2\text{O}_5^b$
Whole period	23 Aug–19 Sept	17 ± 33	7 ± 12	112 ± 218	6 ± 7	33 ± 24	76 ± 61	6.9
Continental (Type Ia)	23–26 Aug	49 ± 58	14 ± 22	264 ± 348	12 ± 9	40 ± 31	119 ± 76	5.3
Marine (Type II)	29 Aug–14 Sept	4 ± 4	2 ± 3	33 ± 36	4 ± 4	22 ± 13	51 ± 43	9.1
Continental (Type Ib)	15–17 Sept	44 ± 39	15 ± 13	269 ± 355	7 ± 10	56 ± 25	138 ± 47	6.1
Continental + Marine (Type III)	27/28 Aug and 18/19 Sept	15 ± 10	8 ± 6	154 ± 135	6 ± 4	52 ± 24	79 ± 53	10.1

^a Similar to Eq. (5), $\tau(\text{N}_2\text{O}_5) = \frac{[\text{N}_2\text{O}_5]}{k_1[\text{NO}_2][\text{O}_3]}$.

^b Mean ratio.

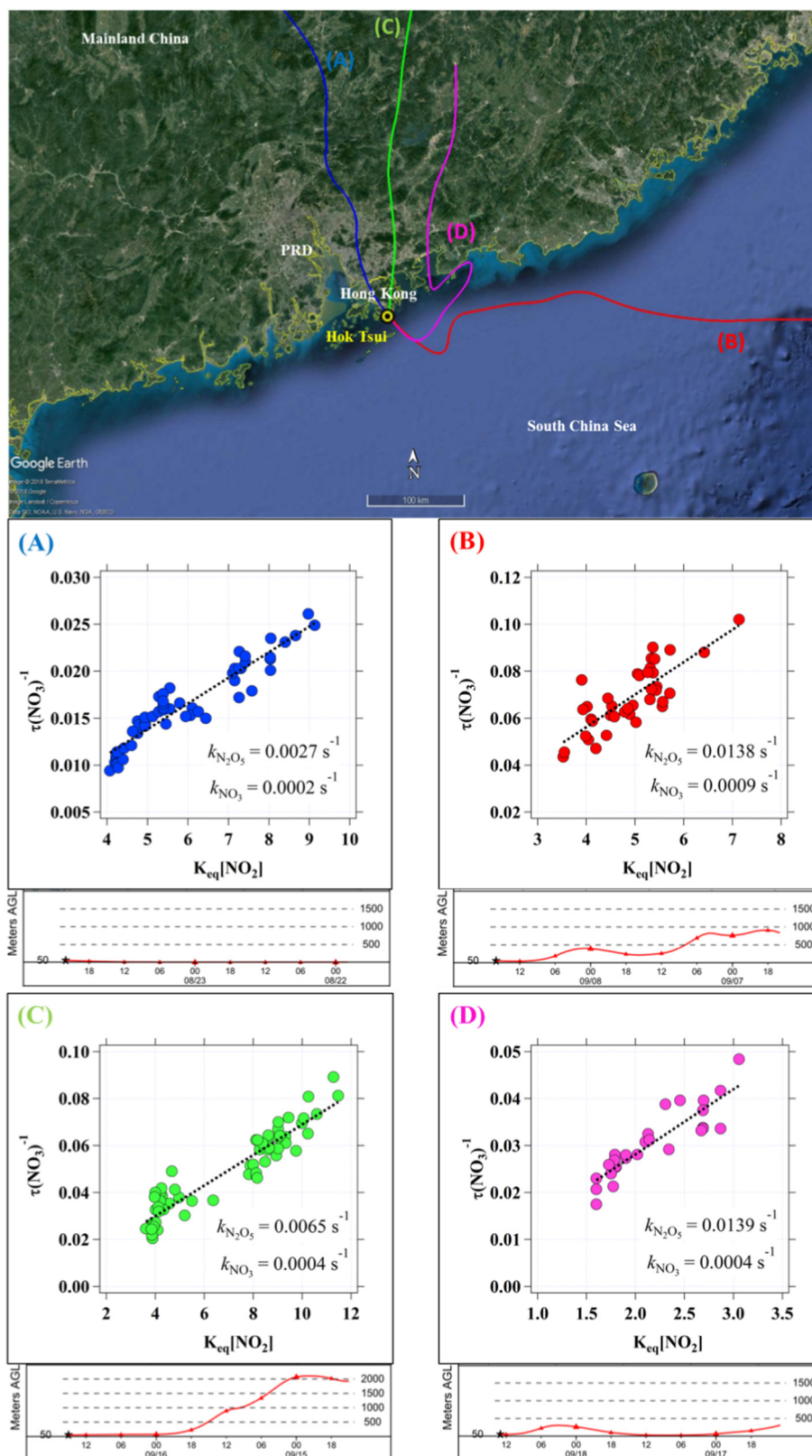


Fig. 4. 48-h back-trajectories calculated from HYSPLIT for four specific nights: (A) 23–24 August, (B) 8–9 September (C) 16–17 September; and (D) 18–19 September. Scatter plots showing the determined loss rates of NO_3 and N_2O_5 using the method described in Section 2.3. Lower panel of each plot shows the height of the air mass before arriving at the sampling site.

heterogeneous reaction has been observed in other marine or coastal environment (e.g., Wood et al., 2005; Aldener et al., 2006; Osthoff et al., 2008; Wagner et al., 2012; Morgan et al., 2015), but the

absolute N_2O_5 heterogeneous loss rates in at our site are considerably faster than most of the rates reported in those studies. For example, measurement in San Francisco bay observed the $k_{\text{N}_2\text{O}_5}$ in the

Table 2
Mean NO_x removal rates and nitrate aerosol formation rates via N₂O₅ heterogeneous reaction during the four cases (\pm standard deviation, 1 σ), as well as their comparison with the adjacent daytime via HNO₃ deposition pathway. The lower and higher limits of N₂O₅ pathway are calculated by assuming a unit or zero production of ClNO₂, respectively; the NO₂ + OH values are higher limit, assuming all gas-phase HNO₃ will deposit on particle surfaces.

Airmass	Via N ₂ O ₅ heterogeneous reaction				Via HNO ₃ deposition	
	$L(\text{NO}_x)_{\text{low}}$ (pptv s ⁻¹)	$P(\text{NO}_3^-)_{\text{low}}$ ($\mu\text{g m}^{-3} \text{h}^{-1}$)	$L(\text{NO}_x)_{\text{high}}$ (pptv s ⁻¹)	$P(\text{NO}_3^-)_{\text{high}}$ ($\mu\text{g m}^{-3} \text{h}^{-1}$)	$L(\text{NO}_x)_{\text{high}}$ (pptv s ⁻¹)	$P(\text{NO}_3^-)_{\text{high}}$ ($\mu\text{g m}^{-3} \text{h}^{-1}$)
Type 1a	0.38 \pm 0.11	3.79 \pm 1.09	0.76 \pm 0.22	7.58 \pm 2.19	1.33 \pm 0.58	13.30 \pm 5.80
Type II	0.15 \pm 0.11	1.52 \pm 1.07	0.29 \pm 0.22	2.90 \pm 2.20	0.87 \pm 0.55	8.63 \pm 5.48
Type 1b	0.36 \pm 0.22	3.62 \pm 2.20	0.72 \pm 0.44	7.24 \pm 4.41	1.14 \pm 0.56	11.39 \pm 5.62
Type III	0.23 \pm 0.10	2.30 \pm 0.96	0.46 \pm 0.20	4.61 \pm 1.98	0.25 \pm 0.20	2.54 \pm 2.02

range of 5.6×10^{-5} to $9.8 \times 10^{-4} \text{ s}^{-1}$ (Wood et al., 2005), while cruise measurements along the United States east coast and Los Angeles basin reported N₂O₅ heterogeneous loss rate in between 10^{-4} and 10^{-3} s^{-1} (Osthoff et al., 2008; Wagner et al., 2012). Morgan et al. (2015) observed a largest $k_{\text{N}_2\text{O}_5}$ of $1 \times 10^{-3} \text{ s}^{-1}$ in a plume during the aircraft measurement near London and English Channel.

Among the airmasses, the marine-influenced airmasses (i.e., Type II and Type III) were determined to have faster N₂O₅ loss rates (see Fig. 4) and larger ClNO₂ to N₂O₅ ratios (see Table 1). In other words, the N₂O₅ heterogeneous loss and production of ClNO₂ were higher when the air parcel interacted with the sea than in those the airmasses originated from the continent urban areas. This implied that the marine environment was more efficient in processing the N₂O₅. It can be seen that

the calculated back trajectories height for the Marine and Continent + Marine airmasses were lower than 500 m at least 6 h before arriving at the site (see Fig. 4), suggesting that the airmass containing N₂O₅ and ClNO₂ had been processed along the surface of the ocean after the sunset. During the transport along the ocean, the N₂O₅ can either being uptake onto the sea-spray to produce ClNO₂, and/or deposit onto the sea surface microlayer leading to the terminal loss of N₂O₅ (Finlayson-Pitts et al., 1989). Previous studies at this site have shown that high chloride concentrations were frequently observed in total suspended particles, PM₁₀ and PM_{2.5} (Cheng et al., 2000; Lai et al., 2007). Given the observation of considerable ClNO₂ concentrations (up to 680 pptv), and higher RH in these types of airmasses, which can promote heterogeneous uptake (Ammann et al., 2013; Brown and Stutz, 2012), we believe that the heterogeneous reaction of N₂O₅ was

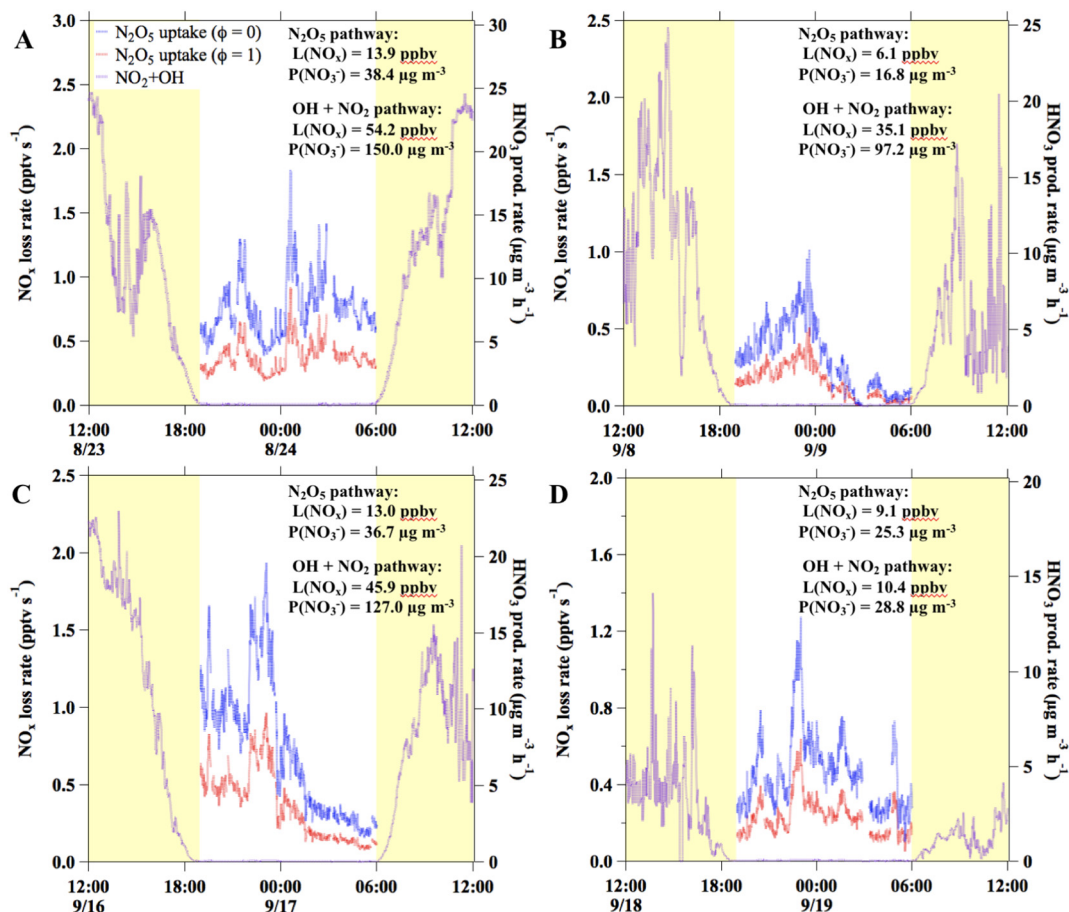


Fig. 5. The NO_x removal rate in pptv s⁻¹ (left axis) and corresponding inorganic nitrate aerosol production rate in $\mu\text{g m}^{-3} \text{h}^{-1}$ (right axis) for a) 23–24 August 2012 (Continent I); b) 8–9 September 2012 (Marine); c) 16–17 September 2012 (Continent II); and d) 18–19 September 2012 (Continent + Marine).

enhanced by the sea-spray/chloride-rich aerosols. However, the importance of N_2O_5 deposition and loss mechanism on the sea surface microlayer is unknown in this region, thereby, more future studies are needed to quantify the roles of air-sea interactions in affecting the N_2O_5 lifetime.

3.3. Nighttime NO_x loss rate

Heterogeneous uptake of N_2O_5 can lead to production of nitrate aerosols and $ClNO_2$ as a cost of NO_x . In this section, we evaluated the potential nighttime NO_x loss from the N_2O_5 heterogeneous uptake. The potential nighttime NO_x removal rate can be calculated by Eq. (8), where the ϕ is the production yield of $ClNO_2$, which will recycle a NO_2 when photolyzed at sunrise. Setting the ϕ to 0 and 1 gives the upper (high) and the lower (low) limit of the NO_x removal rate ($L(NO_x)$) and nitrate aerosol production rate ($P(NO_3^-)$), respectively.

$$L(NO_x) = P(NO_3^-) = (2 - \phi)k_{N_2O_5}[N_2O_5] \quad (8)$$

By using the $k_{N_2O_5}$ determined above and assume that the rate is constant throughout the night, the potential nighttime NO_x removal rates for the 4 examples of airmass types were shown in Table 2.

Since significant levels of $ClNO_2$ has been observed concurrently, the actually NO_x removal rate might be more close to the lower limits, which were 0.38 ± 0.11 and 0.36 ± 0.22 pptv s^{-1} for Type Ia and Ib, 0.15 ± 0.11 pptv s^{-1} for Type II, and 0.23 ± 0.10 pptv s^{-1} for Type III. Although $k_{N_2O_5}$ was lower in continental airmasses than in the marine one, the $L(NO_x)$ and $P(NO_3^-)$ were higher owing to the more abundant N_2O_5 , suggesting that N_2O_5 pathway play a more crucial role in continental airmasses. It is also important to note that, despite the moderate $L(NO_x)$ and $P(NO_3^-)$ in the Type III airmass, the actually influence of such airmass type might be more significant. It is possible that NO_2 , O_3 , and N_2O_5 had experienced efficient losses before reaching our observation station.

We further compared the lower limit of NO_x removal rates via N_2O_5 hydrolysis with the upper limit of main daytime NO_x loss rates assuming that all nitric acid produced via OH oxidation (R1) eventually deposit on surfaces. The OH was calculated using the method described in Section 2.4. Fig. 5 shows the time series of the NO_x removal rates and nitrate aerosol formation rates in the four cases. In the Type Ia and Ib airmasses, N_2O_5 heterogeneous reaction contributed about 20–25% of the NO_x removal and nitrate aerosol formation; this value dropped to 15% in the Type II airmass and increased almost to half in the Type III case. These results are consistent with the study of Yun et al. (2017) that has modeled up to 79% of NO_2 loss in the nocturnal residual layer of Hong Kong was caused by the N_2O_5 heterogeneous reaction. Therefore, we conclude that the N_2O_5 heterogeneous reaction can play a significant role in affecting the NO_x lifetime in this coastal region, especially in the airmasses with continental origins.

4. Summary and conclusions

This study presents a simultaneous measurement of NO_3 , N_2O_5 and $ClNO_2$ using a TD-CIMS at a ground-level coastal site of southern China during the autumn of 2012. During the measurement period, three types of airmasses were determined based on their back trajectories: purely continental air, purely marine air, and marine air with continental origin. Steady-state analysis of N_2O_5 revealed that the overall loss rate of NO_3 and N_2O_5 was high in all four example types of airmasses arriving at the location. In contrast to the finding in the nocturnal residual layer that NO_3 and N_2O_5 have overall similar loss rates (Brown et al., 2016), N_2O_5 loss dominated (>95%) the overall loss and exhibited higher rates in marine air or when the air went across the sea. In such airmasses, faster loss rate of N_2O_5 and higher ratios of $ClNO_2$ to N_2O_5 were also observed compared to continental airmasses,

suggesting stronger heterogeneous reaction of N_2O_5 on chlorine-rich aerosols. Although we did not have the concurrent aerosol measurement, the higher N_2O_5 loss rate might be attributed to several reasons: 1) the chlorine-rich and organic-poor marine aerosols; 2) the higher RH; 3) net deposition on sea surface. The fast loss of N_2O_5 contributed to a significant fraction of NO_x removal and nitrate aerosol formation in this coastal ground-level site. Together with previous studies [Brown et al., 2016; Wang et al., 2016; Yun et al., 2017], the NO_x removal via NO_3 and N_2O_5 pathways can influence the NO_x budget and nitrate formation in a large portion of the planetary boundary layer in the coastal regions of southern China.

Author contributions

Conceptualization, C.Y., Y.J.T. and T.W.; methodology, C.Y., Y.J.T. and X.W.; formal analysis, C.Y., Y.J.T., Q.Z., and J.D.; investigation, C.Y., Y.J.T. and Q.Z.; writing—original draft preparation, C.Y. and Y.J.T.; writing—review and editing, T.W., L.X. and Z.W.; supervision, T.W.; funding acquisition, T.W.

Funding

This work was supported by the Research Grants Council of Hong Kong (A-PolyU502/16).

Acknowledgments

The authors would like to thank Steven Poon, Zheng Xu, Much Yeung and James Chan for logistic support, and assist in preparation of the field studies.

Conflicts of Interest

The authors declare no conflict of interest. The funders had no role in the design of the study; in the collection, analyses, or interpretation of data; in the writing of the manuscript, or in the decision to publish the results.

References

- Aldener, M., Brown, S.S., Stark, H., Williams, E.J., Lerner, B.M., Kuster, W.C., Goldan, P.D., Quinn, P.K., Bates, T.S., Fehsenfeld, F.C., Ravishankara, A.R., 2006. Reactivity and loss mechanisms of NO_3 and N_2O_5 in a polluted marine environment: results from in situ measurements during New England Air Quality Study 2002. *J. Geophys. Res.-Atmos.* 111.
- Ammann, M., Cox, R.A., Crowley, J.N., Jenkin, M.E., Mellouki, A., Rossi, M.J., Troe, J., Wallington, T.J., 2013. Evaluated kinetic and photochemical data for atmospheric chemistry: volume VI – heterogeneous reactions with liquid substrates. *Atmos. Chem. Phys.* 13, 8045–8228. <https://doi.org/10.5194/acp-13-8045-2013>.
- Bertram, T., Thornton, J., 2009. Toward a general parameterization of N_2O_5 reactivity on aqueous particles: the competing effects of particle liquid water, nitrate and chloride. *Atmos. Chem. Phys.* 9, 8351–8363.
- Brown, S.S., Stutz, J., 2012. Nighttime radical observations and chemistry. *Chem. Soc. Rev.* 41, 6405–6447. <https://doi.org/10.1039/c2cs35181a>.
- Brown, S.S., Stark, H., Ravishankara, A.R., 2003a. Applicability of the steady state approximation to the interpretation of atmospheric observations of NO_3 and N_2O_5 . *J. Geophys. Res.-Atmos.* 108, 4539.
- Brown, S.S., Stark, H., Ryerson, T.B., Williams, E.J., Nicks Jr., D.K., Trainer, M., Fehsenfeld, F.C., Ravishankara, A., 2003b. Nitrogen oxides in the nocturnal boundary layer: simultaneous in situ measurements of NO_3 , N_2O_5 , NO_2 , NO , and O_3 . *J. Geophys. Res.-Atmos.* 108.
- Brown, S.S., Ryerson, T.B., Wollny, A.G., Brock, C.A., Peltier, R., Sullivan, A.P., Weber, R.J., Dube, W.P., Trainer, M., Meagher, J.F., Fehsenfeld, F.C., Ravishankara, A.R., 2006. Variability in nocturnal nitrogen oxide processing and its role in regional air quality. *Science* 311, 67–70.
- Brown, S.S., Dube, W.P., Fuchs, H., Ryerson, T.B., Wollny, A.G., Brock, C.A., Bahreini, R., Middlebrook, A.M., Neuman, J.A., Atlas, E., Roberts, J.M., Osthoff, H.D., Trainer, M., Fehsenfeld, F.C., Ravishankara, A.R., 2009. Reactive uptake coefficients for N_2O_5 determined from aircraft measurements during the Second Texas Air Quality Study: comparison to current model parameterizations. *J. Geophys. Res.-Atmos.* 114.
- Brown, S.S., Dubé, W.P., Peischl, J., Ryerson, T.B., Atlas, E., Wameke, C., De Gouw, J.A., te Lintel Hekkert, S., Brock, C.A., Flocke, F., 2011. Budgets for nocturnal VOC oxidation

- by nitrate radicals aloft during the 2006 Texas Air Quality Study. *J. Geophys. Res.-Atmos.* 116.
- Brown, S.S., Dubé, W.P., Tham, Y.J., Zha, Q., Xue, L., Poon, S., Wang, Z., Blake, D.R., Tsui, W., Parrish, D.D., 2016. Nighttime chemistry at a high altitude site above Hong Kong. *J. Geophys. Res.-Atmos.* 121.
- Cheng, Z., Lam, K., Chan, L., Wang, T., Cheng, K., 2000. Chemical characteristics of aerosols at coastal station in Hong Kong. I. Seasonal variation of major ions, halogens and mineral dusts between 1995 and 1996. *Atmos. Environ.* 34, 2771–2783.
- Crowley, J., Thieser, J., Tang, M., Schuster, G., Bozem, H., Beygi, Z.H., Fischer, H., Diesch, J.-M., Drewnick, F., Borrmann, S., 2011. Variable lifetimes and loss mechanisms for NO₃ and N₂O₅ during the DOMINO campaign: contrasts between marine, urban and continental air. *Atmos. Chem. Phys.* 11, 10853.
- Draxler, R.R., Hess, G., 1998. An overview of the HYSPLIT_4 modelling system for trajectories. *Aust. Meteorol. Mag.* 47, 295–308.
- Ehhalt, D.H., Rohrer, F., 2000. Dependence of the OH concentration on solar UV. *J. Geophys. Res.-Atmos.* 105, 3565–3571.
- Finlayson-Pitts, B., Ezell, M., Pitts Jr., J., 1989. Formation of chemically active chlorine compounds by reactions of atmospheric NaCl particles with gaseous N₂O₅ and ClONO₂. *Nature* 337, 241.
- Gaston, C.J., Thornton, J.A., 2016. Reacto-diffusive length of N₂O₅ in aqueous sulfate- and chloride-containing aerosol particles. *J. Phys. Chem. A* 120, 1039–1045.
- Gaston, C.J., Thornton, J.A., Ng, N.L., 2014. Reactive uptake of N₂O₅ to internally mixed inorganic and organic particles: the role of organic carbon oxidation state and inferred organic phase separations. *Atmos. Chem. Phys.* 14, 5693–5707.
- Hahn, J., Luther, K., Troe, J., 2000. Experimental and theoretical study of the temperature and pressure dependences of the recombination reactions O+NO₂(+M) → NO₃(+M) and NO₂+NO₃(+M) → N₂O₅(+M). *Phys. Chem. Chem. Phys.* 2, 5098–5104. <https://doi.org/10.1039/b005756h>.
- Hofzumahaus, A., Rohrer, F., Lu, K., Bohn, B., Brauers, T., Chang, C.-C., Fuchs, H., Holland, F., Kita, K., Kondo, Y., 2009. Amplified trace gas removal in the troposphere. *science* 324, 1702–1704.
- Hoyle, C.R., Boy, M., Donahue, N.M., Fry, J.L., Glasius, M., Guenther, A., Hallar, A.G., Hartz, K.H., Petters, M.D., Petaja, T., Rosenorn, T., Sullivan, A.P., 2011. A review of the anthropogenic influence on biogenic secondary organic aerosol. *Atmos. Chem. Phys.* 11, 321–343. <https://doi.org/10.5194/acp-11-321-2011>.
- Kercher, J., Riedel, T., Thornton, J., 2009. Chlorine activation by N₂O₅: simultaneous, in situ detection of ClNO₂ and N₂O₅ by chemical ionization mass spectrometry. *Atmos. Meas. Tech.* 2, 193–204.
- Lai, S., Zou, S., Cao, J., Lee, S., Ho, K., 2007. Characterizing ionic species in PM_{2.5} and PM₁₀ in four Pearl River Delta cities, South China. *J. Environ. Sci.-China* 19, 939–947.
- Lee, B.H., Mohr, C., Lopez-Hilfiker, F.D., Lutz, A., Hallquist, M., Lee, L., Romer, P., Cohen, R.C., Iyer, S., Kurten, T., Hu, W., Day, D.A., Campuzano-Jost, P., Jimenez, J.L., Xu, L., Ng, N.L., Guo, H., Weber, R.J., Wild, R.J., Brown, S.S., Koss, A., de Gouw, J., Olson, K., Goldstein, A.H., Seco, R., Kim, S., McAvey, K., Shepson, P.B., Starn, T., Baumann, K., Edgerton, E.S., Liu, J., Shilling, J.E., Miller, D.O., Brune, W., Schobesberger, S., D'Ambro, E.L., Thornton, J.A., 2016. Highly functionalized organic nitrates in the southeast United States: contribution to secondary organic aerosol and reactive nitrogen budgets. *Proc. Natl. Acad. Sci. U. S. A.* 113, 1516–1521. <https://doi.org/10.1073/pnas.1508108113>.
- Li, Z., Xue, L., Yang, X., Zha, Q., Tham, Y.J., Yan, C., Louie, P.K., Luk, C.W., Wang, T., Wang, W., 2018. Oxidizing capacity of the rural atmosphere in Hong Kong, Southern China. *Sci. Total Environ.* 612, 1114–1122.
- Lucas, D., Prinn, R., 2005. Parametric sensitivity and uncertainty analysis of dimethylsulfide oxidation in the clear-sky remote marine boundary layer. *Atmos. Chem. and Phys.* 5, 1505–1525.
- Matsumoto, J., Imagawa, K., Imai, H., Kosugi, N., Ideguchi, M., Kato, S., Kajii, Y., 2006. Nocturnal sink of NO_x via NO₃ and N₂O₅ in the outflow from a source area in Japan. *Atmos. Environ.* 40, 6294–6302. <https://doi.org/10.1016/j.atmosenv.2006.05.045>.
- McDuffie, E.E., Fibiger, D.L., Dubé, W.P., Lopez-Hilfiker, F., Lee, B.H., Thornton, J.A., Shah, V., Jaeglé, L., Guo, H., Weber, R.J., 2018. Heterogeneous N₂O₅ uptake during winter: aircraft measurements during the 2015 WINTER campaign and critical evaluation of current parameterizations. *J. Geophys. Res.-Atmos.* 123, 4345–4372.
- Morgan, W.T., Ouyang, B., Allan, J.D., Aruffo, E., Di Carlo, P., Kennedy, O.J., Lowe, D., Flynn, M.J., Rosenber, P.D., Williams, P.I., Jones, R., McFiggans, G.B., Coe, H., 2015. Influence of aerosol chemical composition on N₂O₅ uptake: airborne regional measurements in northwestern Europe. *Atmos. Chem. Phys.* 15, 973–990. <https://doi.org/10.5194/acp-15-973-2015>.
- Ng, N.L., Brown, S.S., Archibald, A.T., Atlas, E., Cohen, R.C., Crowley, J.N., Day, D.A., Donahue, N.M., Fry, J.L., Fuchs, H., Griffin, R.J., Guzman, M.I., Herrmann, H., Hodzic, A., Iinuma, Y., Jimenez, J.L., Kiendler-Scharr, A., Lee, B.H., Lueken, D.J., Mao, J.Q., McLaren, R., Muttel, A., Osthoff, H.D., Ouyang, B., Picquet-Varrault, B., Platt, U., Pye, H.O.T., Rudich, Y., Schwantes, R.H., Shiraiwa, M., Stutz, J., Thornton, J.A., Tilgner, A., Williams, B.J., Zaveri, R.A., 2017. Nitrate radicals and biogenic volatile organic compounds: oxidation, mechanisms, and organic aerosol. *Atmos. Chem. Phys.* 17, 2103–2162. <https://doi.org/10.5194/acp-17-2103-2017>.
- Osthoff, H.D., Roberts, J.M., Ravishankara, A., Williams, E.J., Lerner, B.M., Sommariva, R., Bates, T.S., Coffman, D., Quinn, P.K., Dibb, J.E., 2008. High levels of nitryl chloride in the polluted subtropical marine boundary layer. *Nat. Geosci.* 1, 324.
- Ramanathan, V., Crutzen, P., Kiehl, J., Rosenfeld, D., 2001. Aerosols, climate, and the hydrological cycle. *science* 294, 2119–2124.
- Riedel, T., Bertram, T., Ryder, O., Liu, S., Day, D., Russell, L., Gaston, C., Prather, K., Thornton, J., 2012. Direct N₂O₅ reactivity measurements at a polluted coastal site. *Atmos. Chem. Phys.* 12, 2959–2968.
- Rollins, A.W., Kiendler-Scharr, A., Fry, J.L., Brauers, T., Brown, S.S., Dorn, H.P., Dubé, W.P., Fuchs, H., Mensah, A., Mentel, T.F., Rohrer, F., Tillmann, R., Wegener, R., Wooldridge, P.J., Cohen, R.C., 2009. Isoprene oxidation by nitrate radical: alkyl nitrate and secondary organic aerosol yields. *Atmos. Chem. Phys.* 9, 6685–6703. <https://doi.org/10.5194/acp-9-6685-2009>.
- Ryder, O.S., Ault, A.P., Cahill, J.F., Guasco, T.L., Riedel, T.P., Cuadra-Rodriguez, L.A., Gaston, C.J., Fitzgerald, E., Lee, C., Prather, K.A., 2014. On the role of particle inorganic mixing state in the reactive uptake of N₂O₅ to ambient aerosol particles. *Environ. Sci. Technol.* 48, 1618–1627.
- Slusher, D.L., Huey, L.G., Tanner, D.J., Flocke, F.M., Roberts, J.M., 2004. A thermal dissociation-chemical ionization mass spectrometry (TD-CIMS) technique for the simultaneous measurement of peroxyacyl nitrates and dinitrogen pentoxide. *J. Geophys. Res.-Atmos.* 109.
- Tang, M., Huang, X., Lu, K., Ge, M., Li, Y., Cheng, P., Zhu, T., Ding, A., Zhang, Y., Gligorovski, S., 2017. Heterogeneous reactions of mineral dust aerosol: implications for tropospheric oxidation capacity. *Atmos. Chem. Phys.* 17, 11727–11777.
- Thaler, R.D., Mielke, L.H., Osthoff, H.D., 2011. Quantification of nitryl chloride at part per trillion mixing ratios by thermal dissociation cavity ring-down spectroscopy. *Anal. Chem.* 83, 2761–2766.
- Tham, Y.J., Yan, C., Xue, L.K., Zha, Q.Z., Wang, X.F., Wang, T., 2014. Presence of high nitryl chloride in Asian coastal environment and its impact on atmospheric photochemistry. *Chin. Sci. Bull.* 59, 356–359. <https://doi.org/10.1007/s11434-013-0063-y>.
- Tham, Y.J., Wang, Z., Li, Q., Yun, H., Wang, T., 2016. Significant concentrations of nitryl chloride sustained in the morning: investigations of the causes and impacts on ozone production in a polluted region of northern China. *Atmos. Chem. Phys.* 16, 1–34.
- Tham, Y.J., Wang, Z., Li, Q., Wang, W., Wang, X., Lu, K., Ma, N., Yan, C., Kecorius, S., Wiedensohler, A., 2018. Heterogeneous N₂O₅ uptake coefficient and production yield of ClNO₂ in polluted northern China: roles of aerosol water content and chemical composition. *Atmos. Chem. Phys.* 18, 13155–13171.
- Viggiano, A., Davidson, J., Fehsenfeld, F., Ferguson, E., 1981. Rate constants for the collisional dissociation of N₂O₅ by N₂. *J. Chem. Phys.* 74, 6113–6125.
- Wagner, N., Riedel, T., Roberts, J., Thornton, J., Angevine, W., Williams, E., Lerner, B., Vlasenko, A., Li, S., Dube, W., 2012. The sea breeze/land breeze circulation in Los Angeles and its influence on nitryl chloride production in this region. *J. Geophys. Res.-Atmos.* 117.
- Wang, T., Lam, K., Lee, A.S., Pang, S., Tsui, W., 1998. Meteorological and chemical characteristics of the photochemical ozone episodes observed at Cape D'Aguiar in Hong Kong. *J. Appl. Meteorol. Climatol.* 37, 1167–1178.
- Wang, T., Ding, A., Blake, D., Zahorowski, W., Poon, C., Li, Y., 2003. Chemical characterization of the boundary layer outflow of air pollution to Hong Kong during February–April 2001. *J. Geophys. Res.-Atmos.* 108.
- Wang, T., Guo, H., Blake, D., Kwok, Y., Simpson, I., Li, Y., 2005. Measurements of trace gases in the inflow of South China Sea background air and outflow of regional pollution at Tai O, Southern China. *J. Atmos. Chem. Phys.* 5, 2925.
- Wang, T., Ding, A., Gao, J., Wu, W.S., 2006. Strong ozone production in urban plumes from Beijing, China. *Geophys. Res. Lett.* 33.
- Wang, T., Wei, X.L., Ding, A.J., Poon, C.N., Lam, K.S., Li, Y.S., Chan, L.Y., Anson, M., 2009. Increasing surface ozone concentrations in the background atmosphere of Southern China, 1994–2007. *Atmos. Chem. Phys.* 9, 6217–6227. <https://doi.org/10.5194/acp-9-6217-2009>.
- Wang, T., Nie, W., Gao, J., Xue, L., Gao, X., Wang, X., Qiu, J., Poon, C., Meinardi, S., Blake, D., 2010. Air quality during the 2008 Beijing Olympics: secondary pollutants and regional impact. *Atmos. Chem. Phys.* 10, 7603–7615.
- Wang, X., Wang, T., Yan, C., Tham, Y.J., Xue, L., Xu, Z., Zha, Q., 2014. Large daytime signals of N₂O₅ and NO₃ inferred at 62 amu in a TD-CIMS: chemical interference or a real atmospheric phenomenon. *Atmos. Meas. Tech.* 7, 1–12.
- Wang, T., Tham, Y.J., Xue, L., Li, Q., Zha, Q., Wang, Z., Poon, S.C.N., Dubé, W.P., Blake, D.R., Louie, P.K.K., Luk, C.W.Y., Tsui, W., Brown, S.S., 2016. Observations of nitryl chloride and modeling its source and effect on ozone in the planetary boundary layer of southern China. *J. Geophys. Res.-Atmos.* 121, 2476–2489. <https://doi.org/10.1002/2015jd024556>.
- Wang, H., Lu, K., Chen, X., Zhu, Q., Chen, Q., Guo, S., Jiang, M., Li, X., Shang, D., Tan, Z., Wu, Y., Wu, Z., Zou, Q., Zheng, Y., Zeng, L., Zhu, T., Hu, M., Zhang, Y., 2017a. High N₂O₅ concentrations observed in urban Beijing: implications of a large nitrate formation pathway. *Environ. Sci. Technol. Lett.* 4, 416–420. <https://doi.org/10.1021/acs.estlett.7b00341>.
- Wang, X., Wang, H., Xue, L., Wang, T., Wang, L., Gu, R., Wang, W., Tham, Y.J., Wang, Z., Yang, L., Chen, J., Wang, W., 2017b. Observations of N₂O₅ and ClNO₂ at a polluted urban surface site in North China: high N₂O₅ uptake coefficients and low ClNO₂ product yields. *Atmos. Environ.* 156, 125–134. <https://doi.org/10.1016/j.atmosenv.2017.02.035>.
- Wang, Z., Wang, W., Tham, Y.J., Li, Q., Wang, H., Wen, L., Wang, X., Wang, T., 2017c. Fast heterogeneous N₂O₅ uptake and ClNO₂ production in power plant and industrial plumes observed in the nocturnal residual layer over the North China Plain. *Atmos. Chem. Phys.* 17, 12361–12378. <https://doi.org/10.5194/acp-17-12361-2017>.
- Wood, E., Bertram, T., Wooldridge, P., Cohen, R., 2005. Measurements of N₂O₅, NO₂, and O₃ east of the San Francisco Bay. *Atmos. Chem. Phys.* 5, 483–491.
- Xu, Z., Wang, T., Xue, L., Louie, P.K., Luk, C.W., Gao, J., Wang, S., Chai, F., Wang, W., 2013. Evaluating the uncertainties of thermal catalytic conversion in measuring atmospheric nitrogen dioxide at four differently polluted sites in China. *Atmos. Environ.* 76, 221–226.
- Xue, L., Gu, R., Wang, T., Wang, X., Saunders, S., Blake, D., Louie, P.K., Luk, C.W., Simpson, I., Xu, Z., 2016. Oxidative capacity and radical chemistry in the polluted atmosphere of

- Hong Kong and Pearl River Delta region: analysis of a severe photochemical smog episode. *Atmos. Chem. Phys.* 16, 9891–9903.
- Yan, C., Nie, W., Aijala, M., Rissanen, M.P., Canagaratna, M.R., Massoli, P., Junninen, H., Jokinen, T., Sarnela, N., Hame, S.A.K., Schobesberger, S., Canonaco, F., Yao, L., Prevot, A.S.H., Petaja, T., Kulmala, M., Sipila, M., Worsnop, D.R., Ehn, M., 2016. Source characterization of highly oxidized multifunctional compounds in a boreal forest environment using positive matrix factorization. *Atmos. Chem. Phys.* 16, 12715–12731. <https://doi.org/10.5194/acp-16-12715-2016>.
- Yun, H., Wang, T., Wang, W., Tham, Y.J., Li, Q., Wang, Z., Poon, S., 2017. Nighttime NO_x loss and ClNO₂ formation in the residual layer of a polluted region: insights from field measurements and an iterative box model. *Sci. Total Environ.* 622–623, 727.